Transport in Polygonal Billiards

Daniel Alonso, A. Ruiz and I. de Vega

Departamento de Física Fundamental y Experimental, Electrónica y Sistemas. Universidad de La Laguna. La Laguna 38203, Tenerife, Spain

Abstract

We present in this work a numerical study of the dynamics of ensembles of point particles within a polygonal billiard chain. This billiard is a system with no exponential instability. Our numerical results suggest that some members of the family exhibit normal diffusive behaviour while others present anomalous diffusion. Our conclusions are drawn from the numerical evaluation of the mean square displacement, the velocity autocorrelation function and its spectral analysis. Furthermore we analyze the properties of the incoherent scattering function. The super Burnett coefficient seems to be ill defined in all systems. The multifractal analysis of the spectrum of the velocity autocorrelation functions is also reported. Finally we study the heat conduction in our polygonal chain.

Key words: Polygonal Billiards, Transport Properties, Heat Conduction
PACS: 05.45-a, 05.20.-y, 05.60.Cd, 44.10.+i

1 Introduction

In the last years several works have shed light on our understanding of the connections between transport and dynamical properties. The most relevant results emphasize the role of dynamical chaos in the appearance of normal transport in a dynamical system. In particular the relations between diffusion and quantities as the Kolmogorov-Sinai entropy and the Lyapunov exponents [1–5,**?**,7–9]. Furthermore, the Chaotic hypothesis, which describe non-equilibrium phenomena, has been formulated for a class of hyperbolic systems, the so called transitive Anosov [10]. The common conclusion in all these works is that the stochasticity is required to describe irreversible phenomena and also that relaxation comes from the exponential instability of the microscopic dynamics.

Email addresses: `dalonso@ull.es` (Daniel Alonso,), `antruiz@ull.es` (A. Ruiz).

In general, it is a non trivial question to establish the necessary conditions that a microscopic dynamics should have in order to observe normal transport at macroscopic scale. In this respect, a series of recent works indicate that dynamical systems with dynamical stochasticity weaker than in chaotic systems may show normal transport [11–14]. Furthermore, there are numerical evidences which show that a class of triangular billiards may be mixing [15,16]. All these results encourage a detail study of a class of dynamical systems which may exhibit normal transport although no dynamical chaos is present.

In this paper we report our results on the dynamics of a particle confined in a polygonal billiard table [17]. The main feature of this system is that there is no exponential instability. Therefore it is interesting to study the transport properties of such system. To this aim we shall numerically compute several quantities related to transport such as the mean square displacement and higher order spatial fluctuations. As it is well known in linear response theory, the Green-Kubo formula gives a relation between the diffusion coefficient and the integrated velocity autocorrelation function [18]. In this regard, we will pay special attention to the behaviour of the velocity autocorrelation function and its spectral function by analysing its correlation and information dimensions. We continue with the analysis of the dispersion relation of the hydrodynamic modes [19]. We will also evaluate the Fourier transform of the particle density of the system for long wavelengths (the intermediate incoherent scattering function [20]). Finally we investigate the heat conduction in these systems.

To summarize, we present in this work an analysis of the dynamics in a class of irrational polygons. We are particularly concerned for the possible transport properties that these billiards may exhibit, such as diffusion, correlation decay and heat transport. We continue in this way our previous work on heat conduction in the Lorentz channel [21].

2 The system

Since our main interest is to study transport properties and their relation to specific dynamical properties we consider a point particle confined to move inside a periodic chain. The fundamental cell D of the chain is a polygon in the Euclidean plane $(x, y) = \Re^2$. The border of the cell, ∂D, is composed of straight lines. On the bottom, along the x-axis, there is a saw structure with four equal lines forming two identical edges of angle $\pi - 2\phi_2$. On the top there are two equal segments forming an edge of angle $\pi - 2\phi_1$. The length of the cell along the x-axis is $2d$ and h along the y-axis. Our billiard is constructed by translations of D along the x-axis. In figure (1) we show an schematic representation of the geometry of our system.

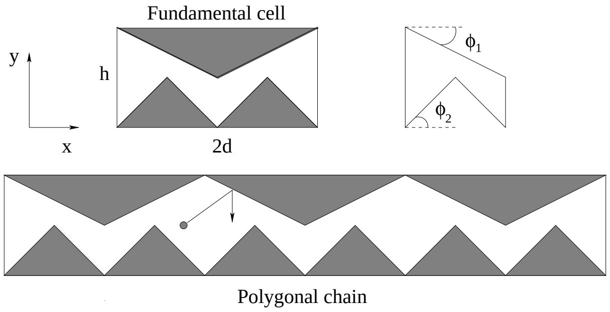

Fig. 1. Schematic representation of the polygonal billiard chain and its parameters. The fundamental cell D is also shown.

We will be mainly concerned for *irrational* polygons, in which at least one angle is irrationally related to π. If all angles are rationally related to π then the polygon it is said to be *rational*.

Associated with the billiard table there is a flow $\Phi^t(-\infty < t < \infty)$ in the phase space $\hat{\Gamma} \equiv (x, y, p_x, p_y)$, where (p_x, p_y) is the momentum of the particle. The conservation of energy confines the motion to a three dimensional restriction of $\hat{\Gamma}$, *i.e.* $\Gamma \equiv (x, y, \theta) = D \times S^1$, where θ is the angle of the velocity measured counterclockwise from the positive x-axis. The problem scales with energy and therefore we can take the velocity such as $|\mathbf{v}| = 1$. The flow Φ^t preserves the measure $dxdyd\theta$. Within the billiard the particle moves freely and suffers elastic collisions at ∂D. The boundary can be parametrized by the arclength s with resp ect to some origin O. Each collision point is labelled by the impact coordinate s and the projection of the velocity $\mathbf{v}$ with respect to the normal unit vector at the boundary $\mathbf{n}$, *i.e.* $\mathbf{v} \cdot \mathbf{n} = \cos\theta$. The flow Φ^t induces a mapping ϕ (Birkoff's map) between pairs $(s, \cos\theta)$ that preserves the measure $dsd(\cos\theta)$. [1]

[1] If the billiard is rational the dynamics takes place on a surface S of genus $g(S) \geq 1$. S has a non trivial topology, which is a consequence of the singular character of the vector fields that can be constructed for the dynamics and that are derived from the constants of motion that exist [22]. Such vector fields are singular for a rational polygon and hence S is topologically equivalent to a multi-handled sphere. For a simply connected billiard of n rational angles, $\alpha_i = \pi p_i/q_i (i = 1, \ldots, n)$, it is possible to give an explicit formula for $g(S)$. Let N be the least common multiple of q_i, then $g(S) = 1 + N/2 \sum_{i=1}^{n}(p_i - 1)/q_i$ [23]. An example of multiply-connected billiard has been studied in [37]. Trivially, the dynamics is non globally ergodic if $g(S) > 1$. Nonetheless the flow Φ^t can be decomposed into one-parameter family of flows Φ^t_θ on the surface S, with $0 < \theta < \pi/N$. The flows Φ^t_θ are called *directional flows* along the direction θ. For almost all angles they are ergodic [23]. It is also known that for a general polygon of n sides there exists a dense set of ergodic polygons. In fact, if a polygon has an irrational angle such that it admits a superexponential fast rational approximation then the dynamics is ergodic. In this sense it is possible to construct irrational polygons that are ergodic [24].

There is a wide mathematical literature related to rational polygons, in contrast to the much less amount of information available for irrational polygons. However there are numerical studies, specially for triangles, that give some insight into the properties of the dynamics in irrational polygons. Artuso [15] has considered right triangles and shown numerically that these systems are at least weakly mixing, whereas his numerical data is not incompatible with mixing. Casati and Prosen [16] extensively studied general triangles in which all three angles are irrational. Their numerical data strongly suggests that irrational triangles are mixing, with correlation decay which appears to be different to those in the triangular billards analyzed by Artuso. In fact, there is no mathematical theorem that supports or precludes the possibility that irrational triangles are mixing [25].

Our fundamental domain is taken an irrational polygon with $\phi_1 = (\sqrt{5}-1)\pi/8$, $\phi_2 = \pi/q (q = 3, 4, 5, 6, 7, 8, 9)$, $h = 1$ and $d = h/(\tan\phi_1 + \tan\phi_2/2)$. With this choice any particle can travel freely along the chain without colliding with the boundaries of the billiard.

3 Particle diffusion

To study diffusion we consider a system with N (large) particles, such that is possible to define a density $n(x,t)$. The Fick's law establishes a linear *phenomenological* relation between the small gradient $\nabla n(x,t)$ and the mass current $\mathbf{j}(x,t)$, *i.e.*

$$D\nabla n(x,t) = \mathbf{j}, \tag{1}$$

where D is the phenomenological diffusion coefficient (independent of space and time). In the case of large enough systems, and provided that there is local conservation of mass, the density $n(x,t)$ satisfies the diffusion equation

$$\partial_t n = D\nabla^2 n. \tag{2}$$

If all particles are located at $x = x_0$ at certain initial time $t = 0$, then the solution of (2) is

$$n(x,t) = \frac{1}{(4\pi Dt)^{1/2}} e^{-(x-x_0)^2/4Dt}. \tag{3}$$

Assuming that all the particles are initially distributed in the system according to their positions $x_i(t = 0)(i = 1, \ldots N)$ and because of the time evolution they are at positions $x_i(t)$ at later time t, the density $n(x,t)$ can be written as the average over the N particles

$$n(x,t) = \Big\langle \delta(x - [x_i(t) - x_i(0)]) \Big\rangle, \tag{4}$$

whereas its Fourier transform $\hat{n}(k,t)$ can be obtained as

$$\hat{n}(k,t) = \int dk e^{ikx} n(x,t) = \Big\langle e^{ik[x_i(t)-x_i(0)]} \Big\rangle. \tag{5}$$

The function $n(x,t)$ is known, after Van Hove [19], as *self space-time correlation function*, and its Fourier transform $\hat{n}(k,t)$ is called *incoherent intermediate scattering function*. It is obvious that if the self space-time correlation function satisfies the diffusion equation, then the incoherent intermediate scattering function satisfies the diffusion equation in reciprocal space,

$$\partial_t \hat{n}(k,t) = -k^2 D \hat{n}(k,t), \tag{6}$$

with the initial condition $\hat{n}(k,0) = 1$. The resolution of this initial value problem gives:

$$\hat{n}(k,t) = e^{-k^2 Dt}. \tag{7}$$

The diffusion equation can then be written, with the help of equation (5), as a linear superposition of *hydrodynamic modes* spatially periodic with wavenumber k. [2]

$$n_k(x,t) = e^{ikx} e^{-k^2 Dt}. \tag{8}$$

It is convenient for our purposes to introduce, from the incoherent intermediate scattering function, the dispersion relation for the hydrodynamic modes [26]

$$s_k = \lim_{t\to\infty} \frac{1}{t} \ln \hat{n}(k,t) = -k^2 D, \tag{9}$$

in terms of which the hydrodynamic modes are expressed as [9]

$$n_k(x,t) = e^{ikx} e^{s_k t}. \tag{10}$$

The term $\nabla^2 n$ in the diffusion equation is a consequence of a first approximation for the thermodynamic force conjugated to the mass current (Fick's law).

[2] We follow the notation of [9]

If $n(x,t)$ varies rapidly in space, new terms with higher spatial derivatives of such function should be included in (2). The first term to add has the form $B\nabla^4 n$, where B is the super Burnett coefficient. In this case a more general expression for s_k follows

$$s_k = \lim_{t\to\infty} \frac{1}{t} \ln \hat{n}(k,t) = -Dk^2 + Bk^4 + \vartheta(k^6). \tag{11}$$

All this remains valid in the case that B is well defined. An interesting feature of the incoherent intermediate scattering function is its relations to the spatial fluctuations. In particular the relation between its first derivative and the average value of the fluctuation $\Delta x = x(t) - x(0)$,

$$\partial_k \, \hat{n}(k,t)|_{k=0} = \langle \Delta x \rangle, \tag{12}$$

and also the relation between its second derivative and the mean square displacement

$$\partial^2_{kk} \hat{n}(k,t)|_{k=0} = -\langle (\Delta x)^2 \rangle. \tag{13}$$

If the diffusion equation holds it follows the Einstein relation for diffusion

$$\langle (\Delta x)^2 \rangle = 2Dt. \tag{14}$$

In the same manner it is possible to derive relations involving higher order fluctuations. A short calculation gives the explicit formula

$$\langle (\Delta x)^4 \rangle - 3\langle (\Delta x)^2 \rangle^2 = 24Bt, \tag{15}$$

which is an Einstein relation for the super Burnett coefficient.

We speak of *normal diffusion* when the Einstein relation (14) is satified. Otherwise, if the mean square displacement does not grow linearly in time we refer to *anomalous diffusion*.

3.1 Numerical simulations

We start our analysis of the diffusive behavior of our systems by computing the mean square displacement and studying its time variation in order to explore the validity of the Einstein relation for diffusion. Due to the geometry of our system the particles transport is restricted along the x-direction.

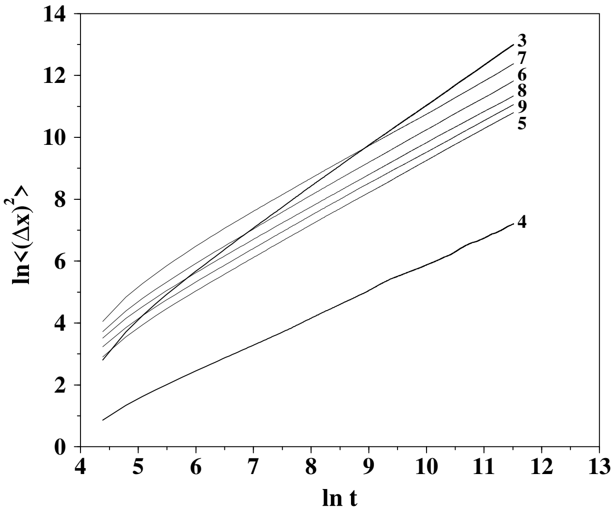

Fig. 2. Mean square displacement of position for $\phi_2 = \pi/q\,(q = 3, 4, 5, 6, 7, 8, 9)$. The label on the right hand side of each curve indicates the value of q. The simulations were done for 1.2×10^5 particles and up to time $t_f = 10^5$. The value of the slope for each curve is indicated in table (1).

We numerically integrated the motion for an ensemble of 1.2×10^5 particles up to $t_f = 10^5$ continuous time units. The mean square displacement was computed from a Monte-Carlo average over the particles. We focused on the cases $\phi_2 = \pi/q$, $q = 3, 4, 5, 6, 7, 8, 9$. Up to the maximum time we have considered, the mean square displacement for the $\phi_2 = \pi/3$ system grows as $\sim t^{1.3}$, which reflects a superdiffusive behavior. The case $\phi_2 = \pi/4$ behaves subdiffusively, with $< (\Delta x)^2 >\sim t^{0.86}$. All the other systems have a power very close to one, from this data we can infer that they satisfy the Einstein relation for diffusion. These results are shown in figure (2) and table (1).

Our numerical results indicate then that the family of systems considered presents both types of diffusive behavior, strange and normal, *at least up to the time we can reach in our simulations.*

As we have previously discussed, an alternative way to characterize the nature of the dynamics of an ensemble of particles is through the analysis of the s_k function (9), where k is the x-component of the wavevector. If the motion is diffusive we should observe that for small values of k the results are compatible with the equation (9).

To clarify this question we took an ensemble of 1.2×10^6 particles and integrated their trajectories up to a time $t_f = 5 \times 10^3$. ¿From the data obtained we constructed the histograms of x-positions as numerical approximation of $n(x, t_f)$. In figure (3) we show the results for the systems $\pi/3$ and $\pi/4$, and in figure (4) the data for the systems $\pi/5$ and $\pi/6$.

ϕ_2	B
$\pi/3$	1.30
$\pi/4$	0.86
$\pi/5$	1.03
$\pi/6$	1.04
$\pi/7$	1.06
$\pi/8$	1.01
$\pi/9$	1.01

Table 1
Diffusion with 1.2×10^5 particles up to a continuous time 10^5. B was obtained from the fitting $< (\Delta x)^2 >= At^B$.

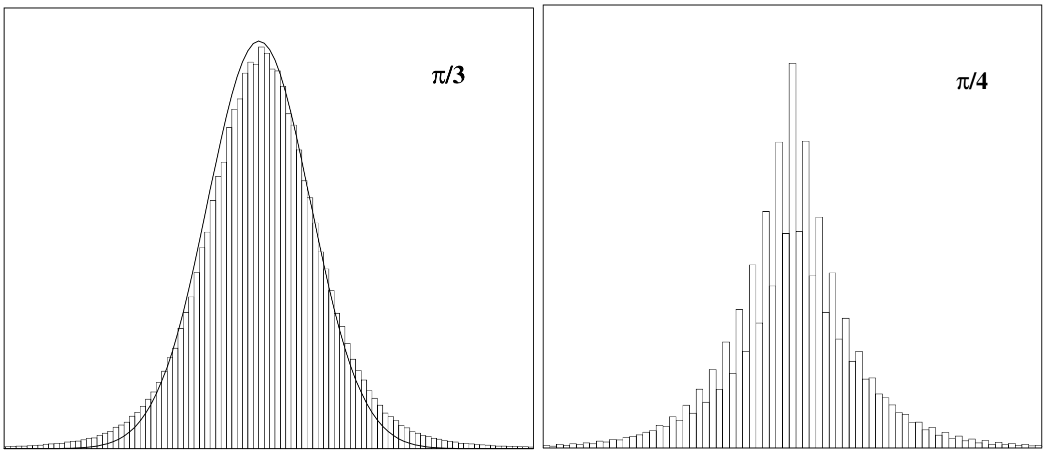

Fig. 3. Histograms of x coordinates for an ensemble of 1.2×10^6 particles at time $t_f = 5 \times 10^3$, for $\phi_2 = \pi/3$ and for $\phi_2 = \pi/4$. The thick line ($\pi/3$) is the best Gaussian fitting to the data.

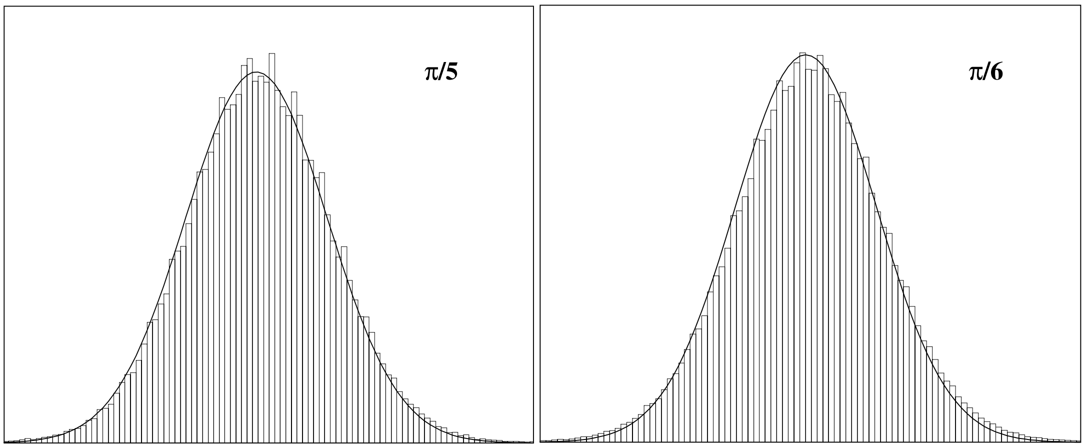

Fig. 4. The same as figure (3) for the systems $\phi_2 = \pi/5$ and $\phi_2 = \pi/6$.

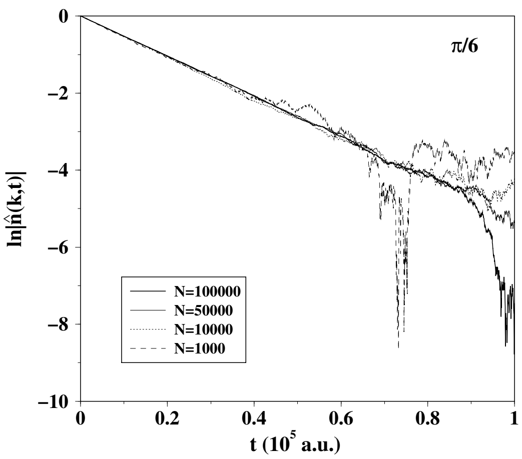

Fig. 5. $ln|\hat{n}(k,t)|$ vs. time for $\phi_2 = \pi/6$, computed with an increasing number of particles N and a fixed value of $k = k_x = 0.01, k_y = 0$.

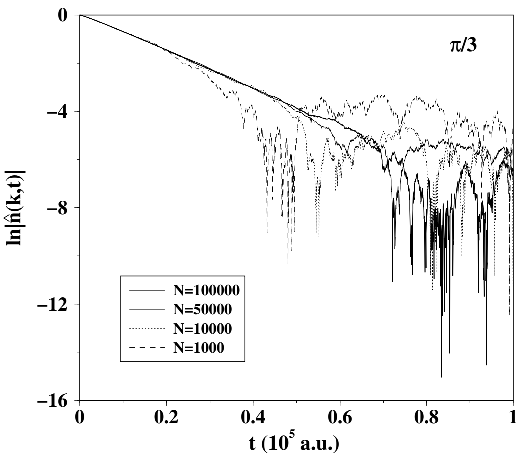

Fig. 6. The same as figure (5) for $\phi_2 = \pi/3$.

The figures also include the best Gaussian fitting (for comparison) of the data. Clearly the $\pi/4$ system is far from a Gaussian shape, while the other systems seem to be closer. The tails of the histograms are very well reproduced by a Gaussian profile for $\phi_2 = \pi/5$ and $\pi/6$, but not for the $\phi_2 = \pi/3$ system, which shows some deviations from the Gaussian bell.

We have computed $\hat{n}(k,t)$ from a series of numerical simulations with an increasing number of particles and a fixed value of $k_x = k = 0.01, k_y = 0$. In all cases it is observed (see figures 5,6,7) that the decay in time of s_k is better reproduced when the simulations involve a larger number of particles. It is not however clear from these curves if such decay is really exponential. In order to clarify this question we computed $\ln|\ln(\hat{n}(k,t))|$, see figure (8). From the data obtained it seems that the decay is not exponential for $\phi_2 = \pi/3$ and $\pi/4$, as it seems to be in the cases $\phi_2 = \pi/q, q = 5, 6, 7, 8, 9$, *at least up to the time we are able to reach in our simulations*. In these last systems our numerical

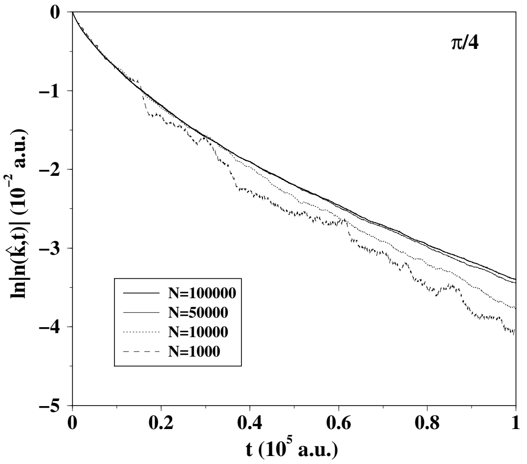

Fig. 7. The same as figure (5) for $\phi_2 = \pi/4$.

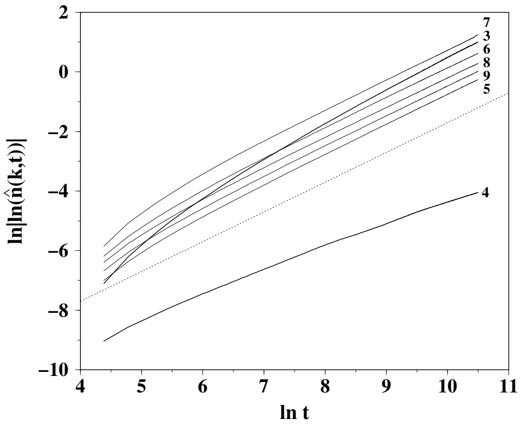

Fig. 8. $\ln|\ln(\hat{n}(k,t))|$ vs. lnt for $\phi_2 = \pi/q$ ($q = 3, 4, 5, 6, 7, 8, 9$). The label on the right hand side of each curve indicates the value of q. The dotted line has slope= 1.

simulations strongly suggest a diffusive behavior and a probable development of hydrodynamic modes.

We could ask ourselves about the super Burnett coefficient in those systems which show diffusive behavior. To analyze this point we considered the particular system $\phi_2 = \pi/6$ and computed $\langle(\Delta x)^4\rangle$ and $3\langle(\Delta x)^2\rangle^2$ from single particle simulations with an increasing length of time discrete series. If the Einstein relation (14) holds and there is a well defined super Burnett coefficient, these two quantities should have the same quadratic growth in time. For this reason, if the curve obtained for $\langle(\Delta x)^4\rangle$ is fitted to the function $\alpha_1 t^2 + \beta_1 t + \gamma_1$, and the one corresponding to $3\langle(\Delta x)^2\rangle^2$ is fitted to the function $\alpha_2 t^2 + \beta_2 t + \gamma_2$, the condition $\alpha_1 = \alpha_2$ must be fulfilled in order to have a well defined Einstein relation for the super Burnett coefficient (15). This would also imply that the difference $\langle(\Delta x)^4\rangle - 3\langle(\Delta x)^2\rangle^2$ should grow linearly in time. We proceeded then to extract the coefficients α_1 and α_2 from the curves obtained for $\langle(\Delta x)^4\rangle$ and $3\langle(\Delta x)^2\rangle^2$.

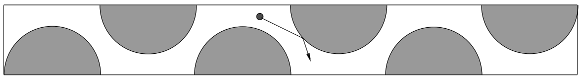

Fig. 9. Schematic representation of a Lorentz channel.

We did the same evaluations for a Lorentz channel (figure 9) [21] in order to have a case to compare with. In this system it is clear that the coefficients α_1 and α_2 get closer as soon as the statistics is improved (see figures 10(a),11). The results for the polygonal chain are drastically different (see figures 10(b),12) and drive us to the conclusion that there is not a well defined super Burnett coefficient for these systems. So we conclude that the polygonal chain has a well defined Einstein relation for diffusion, but not for the super Burnett coefficient. These results were also observed in our ensemble simulations. The fact that the higher moments of Δx are not well defined in a polygonal billiard has been previously studied by Dettmann *et al* [12]. Let us point out that the disorder of the scatterers plays an important role in their results, while in our case the scatterers are ordered [27].

In the escape-rate formalism [8,28] it is important to consider the escape dynamics of the particles from a given region, for instance taking absorbing boundary conditions. The characterization of the escape dynamics can be done by counting the number of particles, $N(t)$, that remains at a given time t inside the selected region. In hyperbolic systems this function decays exponentially in time and the rate of the decay is the so called *escape-rate*. Let us point out that $N(t)$ may present further structure, in the form of oscillations, which are characterized by the Pollicot-Ruelle resonances [29–31]. We have computed $N(t)$ for the cases $\phi_2 = \pi/3$ and $\phi_2 = \pi/6$, propagating 10^5 particles in a system with 50 fundamental boxes, and they do not decay exponentially (see figure (13)). To look closer to this decay we proceed as follows. Let $P(t)\, dt$ be the probability that a particle reaches the boundary at a time within $(t, t + dt)$. It follows that $N(t) = N(0) - \int_0^t P(\tau)d\tau$, from which $P(t) = -dN(t)/dt$. Thus if $N(t)$ decays exponentially so does $P(t)$. The numerical results (see figure (14)) indicate that $P(t)$ does not decay exponentially, and the function $c_0 t^\alpha \exp(-\gamma t^\beta)$ gives a good description of the data, so we expect that $N(t)$ does not decay exponentially in time.

A possible origin of the different diffusive behavior (normal and anomalous) observed in the different members of the family of polygonal billiards could be the set of periodic orbits and propagating modes which may be present in the chain. We have preliminary found that in the case of $\phi = \pi/3$ there is a considerable number of families of propagating modes that contribute to the superdiffusive behavior, these trajectories have a large horizontal component

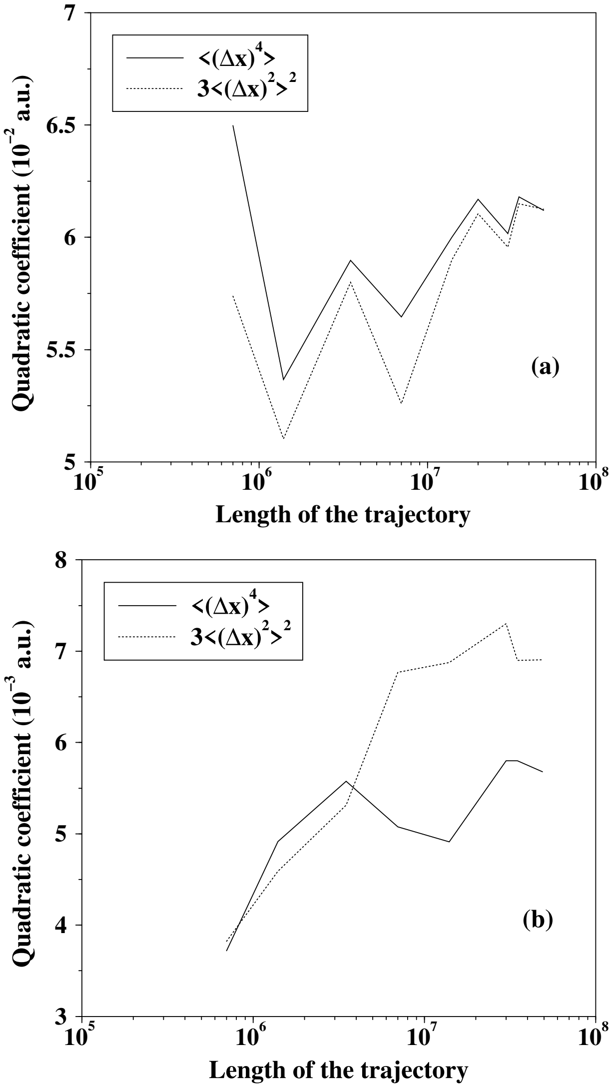

Fig. 10. Coefficients α_1 and α_2 for $3 < (\Delta x)^2 >^2 (t) = \alpha_2 t^2 + \beta_2 t + \gamma_2$ and $< (\Delta x)^4 > (t) = \alpha_1 t^2 + \beta_1 t + \gamma_1$ *.vs.* n (collision time). Figure (a) for the Lorentz-Channel and figure (b) for the polygonal chain.

and a small number of collisions within the cells (see figure (15)). On the other hand in the case $\phi = \pi/4$ it seems that the families of periodic orbits are more abundant that in the case $\phi = \pi/3$. This could explain the subdiffusive behavior (see figure (16)). The system $\phi = \pi/6$ is somehow intermediate, it also has propagating modes (see for example figure (17)), as well as periodic orbits but in small number of families, and furthermore these are propagating modes that present a large number of collisions in the cells without horizontal parts. Certainly this aspect deserves further research.

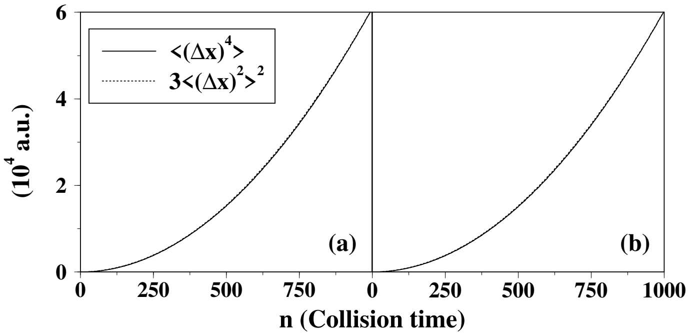

Fig. 11. Comparison of the fluctuation $< (\Delta x)^4 >$ with $3 < (\Delta x)^2 >^2$ for a single particle simulation for the Lorentz channel. Figure (a) is for a time series up to 1.4×10^7 and (b) up to 4.9×10^7 collisions.

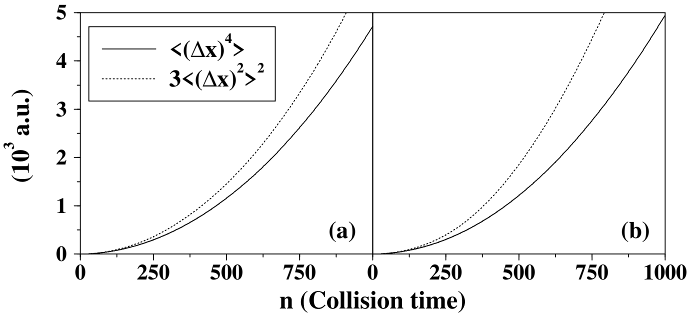

Fig. 12. The same as figure (11) for the polygonal billiard. Figure (a) is for a time series up to 3×10^7 and (b) up to 4.9×10^7 collisions.

4 Velocity autocorrelation function and spectral functions

The behaviour of correlations functions plays an important role in the understanding of transport properties. In particular the velocity autocorrelation (VACF) function is linked to diffusion through the Green-Kubo formula [18].

The velocity autocorrelation function should decay fast enough in order to have a well defined diffusion coefficient, it is then our aim to study the velocity autocorrelation function, in particular its decay and spectral properties. With respect to transport, systems with real continuous spectrum and fast enough decay of correlation functions may present Gaussian fluctuations in their approach to equilibrium, in the sense of the Central Limit Theorem. For such systems it is possible to have a well defined transport coefficient.

Let us consider then a dynamical system (Φ^t, Γ, μ), where Φ^t is a flow (t maybe discrete) acting on a phase space Γ with an invariant measure μ [32]. To study how statistical ensembles evolve in this system we consider correlation

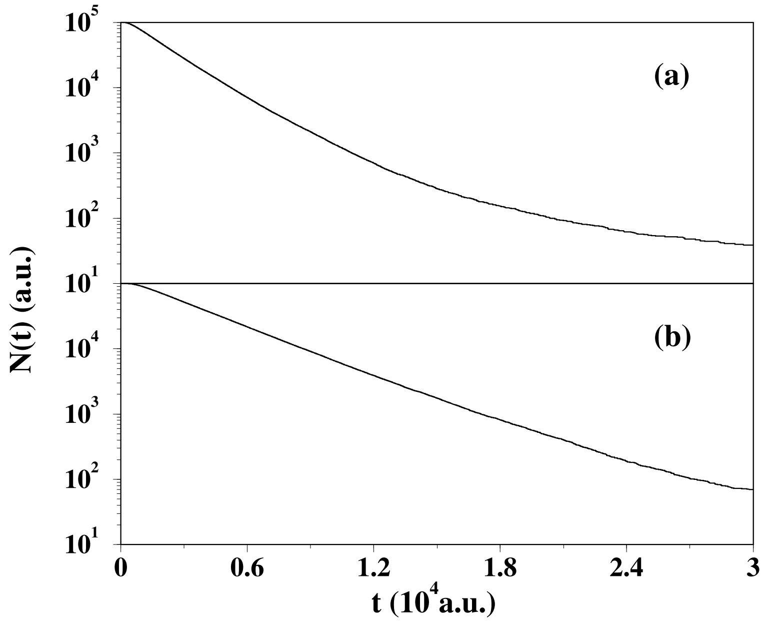

Fig. 13. Typical N(t) functions for the system $\phi_2 = \pi/3$ (figure (a)) and the system $\phi_2 = \pi/6$ (figure (b)).

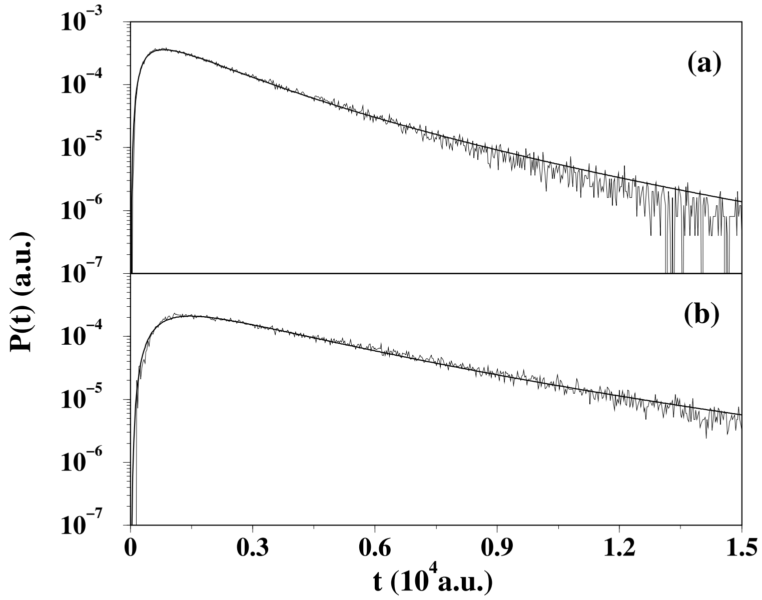

Fig. 14. P(t) functions for the cases $\phi_2 = \pi/3$ (figure (a)) and $\phi_2 = \pi/6$ (figure (b)). The thick line corresponds to the function $c_0 t^\alpha \exp(-\gamma t^\beta)$. In the case of $\phi_2 = \pi/3$ $\alpha = 3.42$ and $\beta = 0.30$ and for $\phi_2 = \pi/6$ $\alpha = 2.39$ and $\beta = 0.44$.

functions such as

$$C^{\Gamma}_{fg} = \int\limits_{\Gamma} d\mu(x) f(\Phi^t x) g(x) - \int\limits_{\Gamma} d\mu(x) f(x) \int\limits_{\Gamma} d\mu(x) g(x). \tag{16}$$

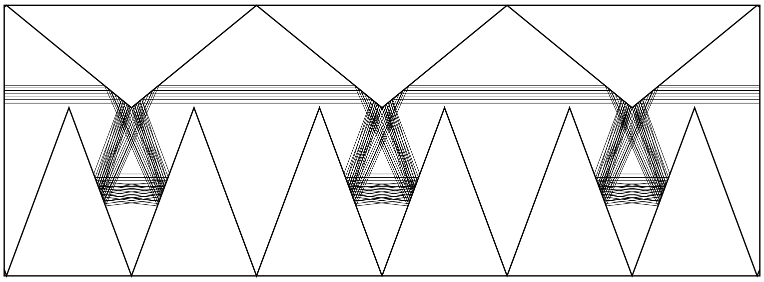

Fig. 15. *Fast propagating mode* in the system $\phi_2 = \pi/3$. This mode is characteristic of this system.

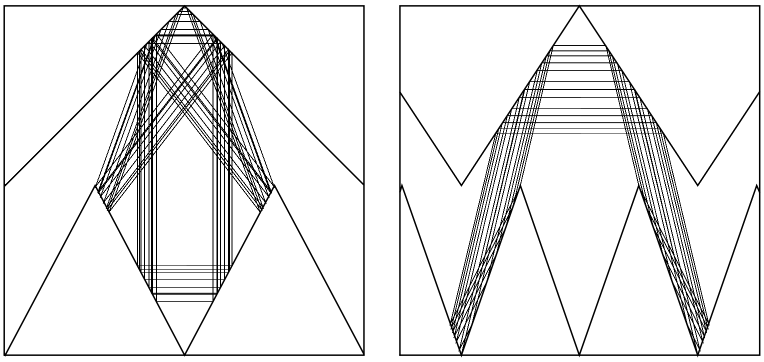

Fig. 16. Typical continuous families of periodic orbits in the system $\phi_2 = \pi/4$.

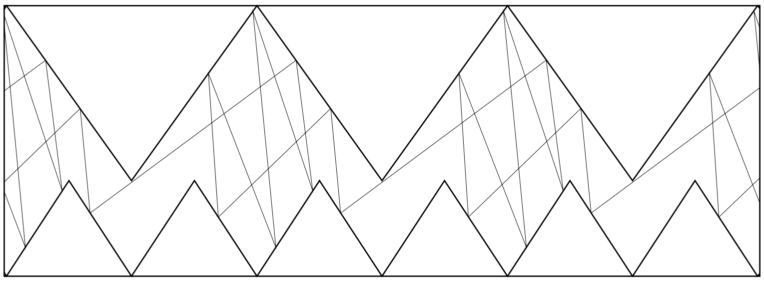

Fig. 17. Typical propagating mode in the case $\phi_2 = \pi/6$.

If they decay to zero for any choice of f and g then we have a system with the mixing property. It is relevant for our purposes to consider the Fourier transform of the correlation function, *i.e.*, the *spectral function*:

$$S_{fg}(\omega) = \int_{-\infty}^{\infty} dt e^{i\omega t} C^{\Gamma}_{fg}(t). \tag{17}$$

The spectral function contains information on how the system evolves in time and which frequencies ω, real or complex, are important in such evolution [33,34]. The complex frequencies are useful to deal with systems that show decay, either exponential or algebraic, which can be characterized in terms of the so called Pollicot-Ruelle resonances. They are also useful in the description of decay properties in chaotic scattering [9,31]. In this article we only consider the real spectrum.

The spectral analysis of a system starts from the *evolution operator* $\hat{U}^t$ acting on the Hilbert space $H = L^2(\Gamma, \mu)$ of square integrable functions, with the scalar product $\langle f|g\rangle = \int_\Gamma f^*(x)g(x)d\mu(x)$. The evolution operator is defined through the action of the flow Φ^t, as $\hat{U}^t f(x) = f(\Phi^t x)$. $\hat{U}^t$ is unitary if Φ^t is invertible and therefore its spectrum is on the unit circle. The properties of the flow can be described in terms of the spectral properties of $\hat{U}^t$. The application of the spectral theorem gives a spectral decomposition of $\hat{U}^t$ in all its components [32,35,36].

In general we have a spectral resolution of $\hat{U}^t$ with the form

$$\hat{U}^t = \int d\hat{E}_\omega e^{-i\omega t} \tag{18}$$

where $\hat{E}_\omega$ is the spectral projector operator corresponding to the real eigenvalue ω. The decomposition is complete in the sense that $\int d\hat{E}_\omega$ is a resolution of the identity.

The nature of the spectrum can be analyzed if we have a realization of a spectral measure associated with a particular observable f within $L^2(\Gamma, \mu)$. The spectral measure associated with f is the inverse Fourier transform of the autocorrelation function of f

$$C^\Gamma_{ff}(t) = \langle f|\hat{U}^t f\rangle = \int \langle f|d\hat{E}_\omega f\rangle e^{-i\omega t} = \int d\mu_f(\omega)e^{-i\omega t}. \tag{19}$$

The nature of the spectrum is contained in $d\mu_f(\omega)$ or its cumulative function

$$\int\limits_{\omega_{min}}^{\omega} d\mu_f(\omega') = F_f(\omega). \tag{20}$$

If for any choice of $f \in H$ the spectrum is continuous then the system is mixing. However, if there is a point spectrum contribution the system cannot be mixing or even weak-mixing. The presence of the weak-mixing property without mixing has been studied and related to the existence of singular continuous components in the spectrum [37].

As it has been mentioned before, a system with continuous spectrum, and for which the autocorrelation function of some observable f decays fast enough, may exhibit Gaussian fluctuations.

A generalized diffusion coefficient, D_f, related to the autocorrelation function

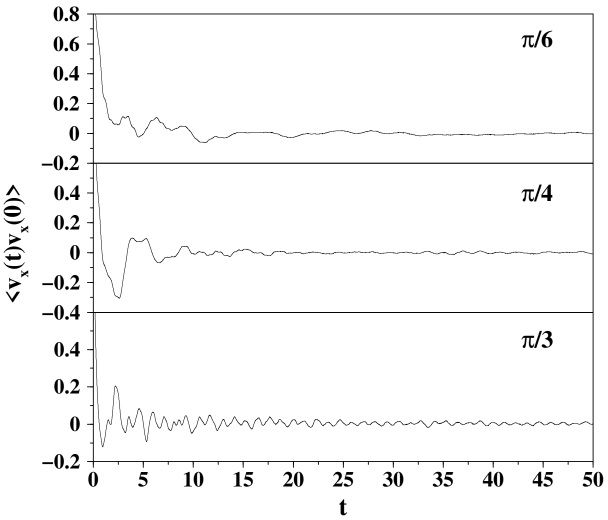

Fig. 18. Velocity autocorrelation functions for $\phi_2 = \pi/6, \pi/4$ and $\pi/3$.

of f by the Green-Kubo formula may be defined

$$D_f = \frac{1}{2} \int_{-\infty}^{\infty} d\tau C^{\Gamma}_{ff}(\tau) \tag{21}$$

with the condition $\lim_{T\to\infty} (1/T) \int_{-T}^{T} d\tau |\tau| C^{\Gamma}_{ff}(\tau) = 0$. In terms of the spectral function $S_{ff}(\omega)$ it follows then

$$2D_f = S_{ff}(0). \tag{22}$$

This equation links the behavior of the short frequency modes with transport, encoded by the generalized diffusion constant D_f at dynamical level.

In figure (18) it is shown the numerical VACF obtained for the systems $\phi_2 = \pi/3, \pi/4$ and $\pi/6$ in numerical simulations with 10^6 particles, initially distributed at random in one fundamental cell, and integrated their trajectories over 2^{15} time steps with $\Delta t = 10^{-2}$. The oscillatory behaviour of the VACF in these systems contrast with the monotonous decay in the Lorentz gas. In figure (19) it is represented the VACF in log-log scale.

As we have already emphasized, the VACF plays an important role in the analysis of diffusion because of the Green-Kubo formula (21). If the VACF decays in a convenient way there exists a well defined diffusion coefficient. In any case, the decay of the VACF can be considered as an indication that the systems treated are mixing. Nonetheless, mixing implies that correlation functions decay for *all* observables and not just for the velocity.

The spectral functions corresponding to the VACF in figure (18) are repre-

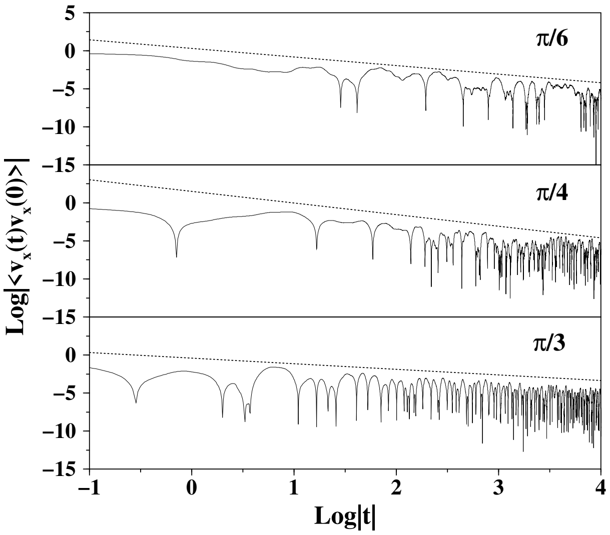

Fig. 19. Absolute value of the velocity autocorrelation functions for $\phi_2 = \pi/6, \pi/4$ and $\pi/3$ in log-log scale. The straight dotted lines have slopes, $\phi_2 = \pi/6(slope = -1.13)$, $\phi_2 = \pi/4(slope = -1.53)$ and $\phi_2 = \pi/3(slope = -0.74)$.

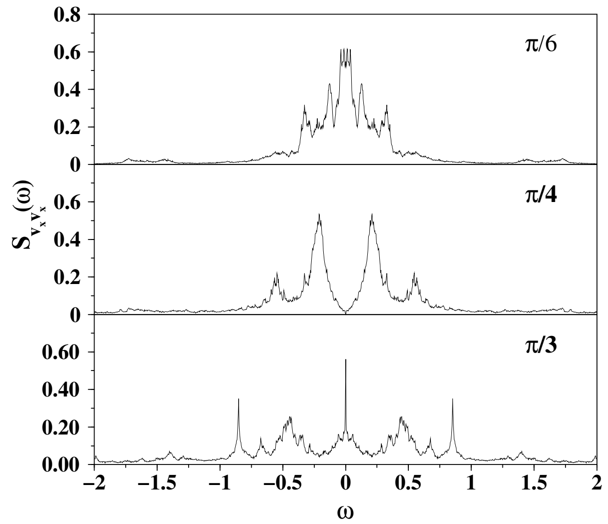

Fig. 20. Spectral functions corresponding to the velocity autocorrelation functions in figure (18).

sented in figure (20). In those systems in which correlations decay a good agreement with equation (22) is observed.

The measure reconstructed from the spectral function may exhibit interesting scaling properties [15,37], in particular the correlation and information dimensions. The generalized dimensions of the measure $d\mu_f(\omega)$, $D_1(\mu_f)$ and $D_2(\mu_f)$, are the scaling exponents defined by:

$$\chi_{1,N} = \sum_{\alpha=1}^{2^N} \mu_f(I_{N,\alpha}) \ln \mu_f(I_{N,\alpha}) \sim -ND_1 \ln 2 \tag{23}$$

$$\chi_{2,N} = \ln \sum_{\alpha=1}^{2^N} \mu_f^2(I_{N,\alpha}) \sim -ND_2 \ln 2, \tag{24}$$

where $I_{N,\alpha}$ defines a partition of the spectral interval into $\alpha = 1, ..., 2^N$ subintervals.

It is known [37] that under certain assumptions D_1 coincides with the Hausdorff dimension of the measure, meanwhile the D_2 coefficient is related to the integrated correlation function. In the case of continuos spectrum the integrated correlation

$$C_f^{int}(t) = \frac{1}{t} \int_0^t d\tau \, |C_f(\tau)|^2 \tag{25}$$

of an observable f is expected to decay to zero as:

$$C_f^{int}(t) \sim t^{-D_2} \tag{26}$$

with D_2 defined in equation (24). The multifractal analysis of the spectral measure obtained (see figures (21,22)) indicates that both, D_1 and D_2, are almost one in all cases. This suggests again that the systems could be mixing.

5 Heat conduction

We also studied the heat conduction in the polygonal chain. In the case of the Lorentz Channel normal heat conductivity is observed [38,21]. We will study in this section in which cases ($\phi_2 \, values$) the heat conduction is normal in our polygonal billiards. Some recent results, [13,14,17], suggest that it is possible to have normal heat conduction in this type of systems. Let us point out that another set of studies has been devoted to one dimensional chains of nonlinear coupled oscillators [39–44].

To induce heat transport in our systems we put two heat reservoirs at the left and right hand sides of the billiard chain (see figure (23)). The heat reservoirs

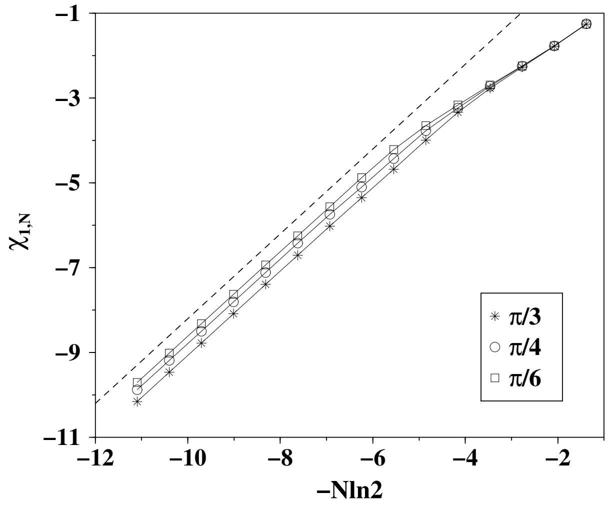

Fig. 21. D_1 coefficient (see text) for the spectrum derived from the velocity auto-correlation function. The dotted line corresponds to a line with slope -1.

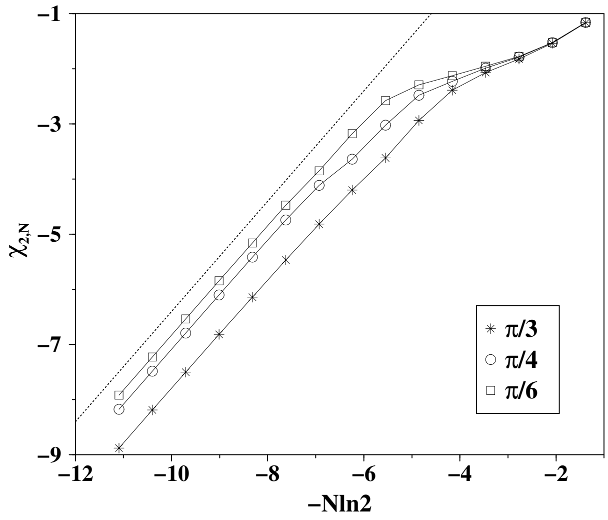

Fig. 22. The same as figure (21) for the coefficient D_2.

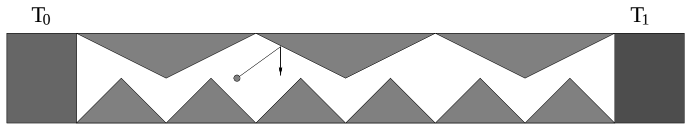

Fig. 23. Schematic representation of a polygonal billiard chain put in contact with two heat reservoirs of temperature T_0 and T_1.

were modelled using stochastic kernels of Gaussian type,

$$P(v) = \pm \frac{|v|}{T} e^{-\frac{v^2}{2T}} \tag{27}$$

where v is the x component of the velocity in the collision with the heat bath at temperature T. The minus sign is taken at the right hand side and the plus sign at the left reservoir. The Boltzmann's constant is set to one.

Following Alonso *et al* [21] we computed the temperature field at the stationary state. To achive this task we defined a grid of points in configuration space $(x_i, y_j), (i = 1, \cdots, N_x, j = 1, \cdots, N_y)$ around which there is a cell C_{ij}. This set of cells defines a partition of the configuration space. During the time evolution the particle crosses the cell C_{ij} in N_{ij} occasions, let us call t_α and $E_\alpha(ij)$ the time spent by the particle and its energy during the α-visit to the cell $(\alpha = 1, \cdots, N_{ij})$. We define a coarse grained temperature field $T(ij)$ as the average

$$T(ij) = \langle E \rangle_{ij} = \frac{\sum_{\alpha=1}^{N_{ij}} t_\alpha E_\alpha(ij)}{\sum_{\alpha=1}^{N_{ij}} t_\alpha}. \tag{28}$$

This procedure defines a two-dimensional field. As we have mentioned the transport takes place along the x direction, so we will focus on the $x - T(x, y)$ plane at some stages.

Another quantity of interest is the heat flux at the stationary state. The kinetic energy is constant within the billiard and only changes when there is a collision with a reservoir, in which case it suffers a change in energy

$$\Delta E_k = E_{in} - E_{out}, \tag{29}$$

with k an index for the collision. If we sum over N of such events that take place over a time t_N we have for the heat flux

$$j_n = \frac{1}{t_N} \sum_{k=1}^{N} \Delta E_k. \tag{30}$$

The stationary state is reached if for long enough time t_N the heat flux is constant.

We numerically computed the temperature field (28), as well as the heat current as a function of the system size. We analyzed how the heat flux scales with the system size. For a single particle simulation and for a system with n fundamental cells (not to be confused with the cells defined for the evaluation of the temperature) we have a flux $j_1(n)$. In order to implement the thermodynamic limit correctly we should study the current $j_n(n) = nj_1(n)$ (for a density of one particle per fundamental cell). In our numerical simulations we

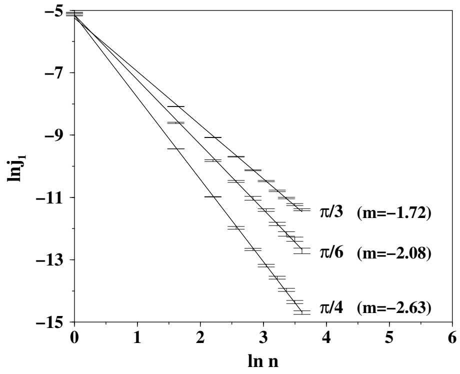

Fig. 24. Scaling behavior of the heat flux for the systems $\phi_2 = \pi/3, \pi/4$ and $\pi/6$. The figures show how the systems $\phi_2 = \pi/3$ and $\pi/4$ have infinite and zero heat conductivity constant respectively while the $\pi/6$-system show a scaling behavior compatible with a well defined heat conductivity coefficient in the Thermodynamic limit. The systems $\phi_2 = \pi/q\,(q = 5, 7, 8, 9)$ have the same behaviour as $\pi/6$. m denotes the slope of each linear fitting (see text).

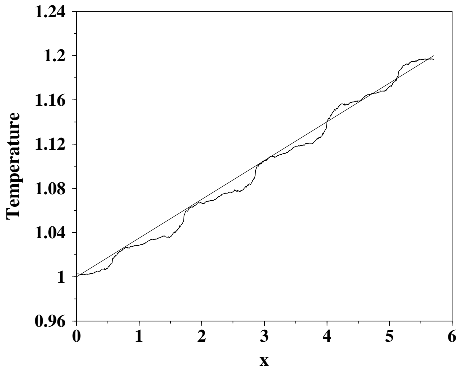

Fig. 25. Temperature profile in the $x - T(x, y)$ plane for a system with $\phi_2 = \pi/6$, five fundamental cells and $T_0 = 1, T_1 = 1.2$. The straight line is the ideal Fourier profile.

found that $j_n(n)$ scales as $\gamma n^{-\delta}$. We have to distinguish the cases $\phi_2 = \pi/3$ and $\phi_2 = \pi/4$ from $\phi_2 = \pi/q\,(q = 5, 6, 7, 8, 9)$.

For $\phi_2 = \pi/3$ is clear that the heat flux is such that leads to an infinite heat conductivity coefficient. In this case $\delta = 0.72$. For $\phi_2 = \pi/4$ the heat current scales with $\delta = 1.63$, what yields a zero heat conductivity coefficient (see figure (24)). All the other systems have scaling exponents very close to one, see [17].

The temperature field (see figure (25)) is linear for small temperature differences and shows some structure induced by the geometry of the boundaries. We can conclude then that for $\phi_2 = \pi/q\,(q = 5, 6, 7, 8, 9)$ the heat conduction is normal, but not for the cases $\phi_2 = \pi/3$ and $\pi/4$, which are superdiffusive and subdiffusive respectively.

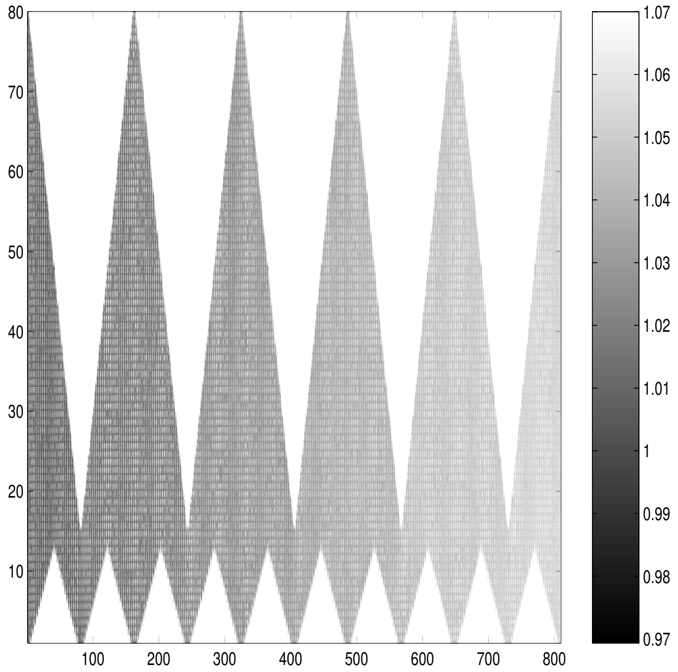

Fig. 26. Density plot of the temperature field for $\phi_2 = \pi/6$, five fundamental cells, $T_0 = 1$ and $T_1 = 1.05$

As notice in [21] the temperature field scales with length as $T_{[0,L]}(x) = T_{[0,1]}(x/L)$. Ifigure (26) we show the typical density plot of the two-dimensional temperature field. In all the systems we have a complete consistency with the results of the diffusive properties of the billiard chain.

6 Conclusions

The different numerical simulations done indicate that the polygonal billiard studied may present normal as well as anomalous diffusion. In any case there is no exponential instability in the dynamics. In the case of the normal diffusive behaviour there is a need to construct a theory in which the exponential instability does not play a role, so another set of ideas are needed to contruct such theory. Our aim in this work has been to compute different quantities to make a careful analysis of the transport properties in the systems studied.

The mean square displacement seems to grow linearly in time for some members of the family studied, but remarkably, for other members it grows either in a subdiffusive or superdiffusive way. The analysis of the dispersion relation for diffusion for long wavelengths has been also explored. We conclude from the analysis of higher order fluctuations of position that the super Burnett coefficient is not well defined in any system.

The computation of the velocity autocorrelation functions and their spectral functions reinforce our conclusion about the transport properties of the polygonal chain. The multifractal analysis of the spectral functions reveals that the Hausdorff dimension of the spectrum is probably one for all systems. The numerical analysis also indicates that the correlation dimension is nearly one.

With regard to the properties of the escape dynamics of our billiards, the number of particles that remain in a finite region in the system at a given time, $N(t)$, decays in time, but not exponentially. In fact the probability $P(t)$ that a particle escapes from the selected region at a given time t is found numerically to be well represented by a function of the form $c_0 t^\alpha \exp(-\gamma t^\beta)$, where β is different from one.

The study of the periodic orbits and propagating modes in the systems studied reveals that those systems that behave subdiffusively have a large number of continuous families of periodic orbits. In contrast, those systems that behave superdiffusively present an important set of families of propagating modes that may be responsible for the supperdiffusive behaviour observed. The other systems are somehow intermediate, notheless our results in this point can only be consider as preliminar.

In the last section we studied the heat conduction in the chain. The temperatures were simulated by stochastic kernels. The conclusion is the expected one, this is, the systems that are diffusive have normal heat transport, and those for which the diffusion is anomalous develop anomalous heat transport.

It remains to study the nature of the non-equilibrium stationary states for diffusion and heat transport, but the fact that the polygonal billiards do not have exponential instability may complicate such analysis. The structure that these non-equilibrium stationary states may develope is an interesting open question.

Finally we would like to stress that we present in this work only numerical results. It would be of great interest to have some conclusive mathematical results on the questions studied in this paper.

7 Acknowledgments

D. Alonso thanks R. Artuso, G. Casati, C. Dettmann, P. Gaspard, I. Guarneri, R. Klages, G. Nicolis, L. Rondoni and H. Van Beijeren for fruitful discussions at different stages of this work at Como, Brussels and Dresden. D. Alonso thanks the warm hospitality of the Max-Planck-Institut Für Physik Komplexer Systeme at Dresden during the workshop on "Microscopic Chaos and Transport in Many-Particle Systems" (August 2002). Support has been provided by the "Ministerio de Ciencia y Tecnología" and FEDER (BFM2001-3349 and BFM2001-3343) and by "Consejería de Educación Cultura y Deportes" (Gobierno de Canarias) under Contract No. PI2002-009. I. de Vega is finantially supported by a Ministerio de Ciencia y Tecnología doctoral fellowship (AP2001-2226).

References

[1] L.A. Bunimovich, Comm. Math. Phys. **65**, 295 (1979). L.A. Bunimovich, Ya. G. Sinai, it ibid **78**, 247 (1980). L.A. Bunimovich, Ya. G. Sinai, it ibid **78**, 479 (1981). L.A. Bunimovich, Physica D, **33**, 58 (1988).

[2] A. Knauf, Commun. Math. Phys. **109**, 1-24 (1987).

[3] L.A. Bunimovich and H. Spohn, Commun. Math. Phys. **176**, 661-680 (1996).

[4] P. Gaspard, J. Stat. Phys., **68**, 673 (1992).

[5] S. Tasaki and P. Gaspard, J. Stat. Phys. **81**, 935, (1995).

[6] R. Artuso, Phys. Lett. A **160**, 528 (1991).

[7] G. Casati and T. Prosen, Phys. Rev. Lett, **85**, 4261-4264 (2000).

[8] J. R. Dorfman and P. Gaspard, Phys. Rev. E **51**, 28 (1995)

[9] P. Gaspard, *Chaos, Scattering and Statistical Mechanics* (Cambridge University Press, 1998).

[10] G. Gallavotti and E.G.D.Cohen, Phys. Rev. Lett, **74**, 2694-2697, (1995), J. Stat. Phys, **80**, 931-970 (1995); G. Gallavotti, J. Stat. Phys, **84**, 899-926, (1996), Phys. Rev. Lett, **77**, 4334-4337, (1996).

[11] S. Lepri, L. Rondoni and G. Benettin, J. Stat. Phys. **99**, 857 (2000) (chao-dyn/9909004). G. Benettin and L. Rondoni, Math. Phys. Electronic Journal, **7(3)**, (2001).

[12] C. P. Dettmann and E. G. D. Cohen and H. Van Beijeren, Nature **401**, 875 (1999). C. P. Dettmann and E. G. D. Cohen, J. Stat. Phys. **101**, 775 (2000).

[13] B. Li, L. Wang and B. Hu, Phys. Rev. Lett., **88**, 223901 (2002).

[14] B. Li, G. Casati and J. Wang, Phys. Rev. E **67**, 021204 (2003).

[15] R. Artuso, Physica D **109**, 1 (1997).

[16] G. Casati and T. Prosen, Phys. Rev. Lett. **83**, 4729 (1999).

[17] Daniel Alonso, A, Ruiz and I. de Vega, Phys. Rev. E **66**, 066131 (2002).

[18] R. Balescu, *Statistical Dynamics* (Imperial College Press, 1997).

[19] L. Van Hove, Phys. Rev. **95**, 249 (1954).

[20] H. Van Beijeren, Rev. Mod. Phys. **54**, 195 (1982).

[21] D. Alonso, R. Artuso, G. Casati and I. Guarneri, Phys. Rev. Lett. **82**, 1859 (1999).

[22] P.J. Richens and M.V. Berry, Physica D **2**, 495-512 (1981).

[23] E. Gutkin, Physica D. **19**, 311-333 (1986).

[24] Ya. Vorobets, Sb. Math. **188**, 389-434 (1997).

[25] E. Gutkin, Max-Planck-Institute für Mathematik in der Naturwissnschaften, Leipzig-preprint 103 (2001).

[26] P. Gaspard and I. Claus, Philosophical Transactions-Royal Society of London Series A Mathematical Physical and Engineering Sciences, vol. 360, no. 1792, pp 303-316 (2002). P. Gaspard, I. Claus, T. Gilbert and J.R. Dorfman, Phys. Rev. Lett. **86**, 1506 (2001).

[27] H. Van Beijeren *private communication.*

[28] P. Gaspard and J. R. Dorfman, Phys. Rev. E **52**, 3525 (1995).

[29] M. Pollicot, Invent. Math. **81**, 413 (1986). M. Pollicot, Invent. Math. **85**, 147 (1986).

[30] D. Ruelle, Phys. Rev. Lett. **56**, 405 (1986).

[31] P. Gaspard and D. Alonso Ramírez, Phys. Rev. A **45**, 8383 (1992).

[32] V. I. Arnold and A. Avez, *Ergodic Problems of Classical Mechanics* (W.A. Benjamin, INC, 1968).

[33] B.O. Koopman, Proc. Natl. Acad. Sci. U.S.A. **17**, 17 (1931).

[34] J. von Neumann, Proc. Natl. Acad. Sci. U.S.A. **18**, 70 (1932).

[35] Ya. G, Sinai (ed.), *Dynamical Systems II* (Encyclopaedia of Mathematical Sciences Vol. 2, Springer Verlag, 1985).

[36] M. Reed and B. Simon, *Methods of Modern Mathematical Physics: I, Functional Analysis* (Academic Press, 1980).

[37] R. Artuso, I. Guarneri and L. Rebuzzini, Chaos **10**, 189 (2000).

[38] J. L. Lebowitz and H. Spohn, J. Stat. Phys. **19**, 633 (1978).

[39] T. Prosen and M. Robnik, J. Phys. A, **25**, 3449-3472, (1992).

[40] D.J.R. Mimnagh and L. E. Ballentine, Phys. Rev. E **56**, 5332-5342, (1997).

[41] G. Casati, J. Ford, F. Vivaldi and W. M. Visscher, Phys. Rev. Lett., **52**, 1861, (1984).

[42] G. Casati and T. Prosen, axXiv:cond-mat/0203331 (2002).

[43] S. Lepri, R. Livi and A. Politi, Phys. Rev. Lett., **78**, 1896, (1997). A.Fillipov, Bambi Hu, Baowen Li and A. Zeltser, J. Phys. A **31**, 7719, (1998). Bambi Hu, Baowen Li and Hong Zhao, Phys. Rev. E **57**, 2992, (1998). H. Kaburaki and M. Machida, Phys. Lett. A **181**, 85, (1993). A. Kato and D. Jou, Phys. Rev. E **64** 052201 (2001).

[44] B. Li and J. Wang, "Anomalous Heat Conduction and Anomalous Diffusion in One Dimensional Systems", Singapoure University, preprint-2002.